

Decomposing the dynamics of heterogeneous delayed networks with applications to connected vehicle systems

Róbert Szalai¹ and Gábor Orosz²

¹*Department of Engineering Mathematics, University of Bristol, Bristol, BS8 1TR, UK*

²*Department of Mechanical Engineering, University of Michigan, Ann Arbor, Michigan 48109 USA*

(Dated: October 3, 2018)

Delay-coupled networks are investigated with nonidentical delay times and the effects of such heterogeneity on the emergent dynamics of complex systems are characterized. A simple decomposition method is presented that decouples the dynamics of the network into node-size modal equations in the vicinity of equilibria. The resulting independent components contain distributed delays that map the spatiotemporal complexity of the system to the time domain. We demonstrate that this new approach can be used to reveal new physical phenomena in heterogeneous vehicular traffic when vehicles are linked via vehicle-to-vehicle (V2V) communication.

PACS numbers: 02.30.Ks, 05.45.Xt, 64.60.aq, 89.75.Kd, 89.40.Bb

The dynamics of delayed networks are in the current interest of research communities in physics, biology and engineering. Applications include neural networks [7, 17, 21], gene regulatory networks [16, 24], semiconductor lasers [11, 30], and traffic systems [25, 26, 32]. In these systems, delays arise in the couplings between components due to finite-time information propagation, which greatly influence the arising patterns of activity. However, in the above cases it has been assumed that the delays are identical. This is clearly not the case in physical systems, where communication channels have different transmission rates and information travels greatly varying distances. In this Rapid Communication, we characterize the behavior of realistic heterogeneous delayed systems about equilibria by applying a simple decomposition method. In particular, we analyze the dynamics of a connected vehicle system and show that having an optimal level of delay heterogeneity may maximize stability of the uniform flow which has significant implications on traffic dynamics.

In order to understand the system-level behavior arising through delayed connectivity, large systems of delay differential equations have to be analyzed. Even in the absence of delays, one needs to handle high-dimensional systems. Moreover, delays make the dynamics infinite dimensional which typically leads to complicated dynamics even for simple systems. For the case of identical delays, decomposition methods have been proposed [9, 11, 13, 14, 20, 21] to investigate the dynamics in the vicinity of the synchronized equilibrium, which result in (linear autonomous) delayed modal equations of small size. The decomposition methods have been extended to handle the dynamics in the vicinity of synchronous periodic orbits using Floquet theory [21] and synchronous chaos using Lyapunov exponents [18]. Further developments allow decomposition of the dynamics in the vicinity of steady and oscillatory cluster states [10, 22] and the analysis of traveling wave solutions [17]. However, networks with heterogeneous delays escaped many attempts of modal decomposition, because no finite dimensional transformation can untangle the interaction of noniden-

tical delays. As a first step, in this Rapid Communication we propose a simple approach that can handle heterogeneous delays in the vicinity of equilibria at the linear level. The key idea is to decompose the system in the Laplace domain and then transform the uncoupled modal equations back to the time domain. This results in delayed modal equations with distributed delays where the spatiotemporal complexity of the original coupled system is mapped to the time domain by the delay distributions.

As a motivating example we consider a simple, but heterogeneous car-following model [12, 25, 32] where the interaction of vehicles is facilitated by automatic control that is based on wireless vehicle-to-vehicle (V2V) communication [8, 28]. As different channels of information exchange have naturally different delay times, this model is unsuitable for available modal decomposition techniques. By applying our method, we illustrate how individual delays are mixed in the decomposed system. The corresponding modes are traveling wave-like solutions that become traveling waves of different wave lengths in the case of identical delays and next-neighbor interactions [23, 26]. Synthesizing the results obtained for individual traffic modes, we develop a systematic understanding of heterogeneous traffic dynamics for our simple example. The presented method may be used to develop control strategies for larger systems involving V2V communication.

We consider a general description of dynamics on a network written in the form of

$$\dot{x}_i(t) = f(x_i(t)) + \sum_{j=1}^N a_{ij} g(x_i(t), x_j(t - \tau_{ij})), \quad (1)$$

for $i = 1, \dots, N$, where the state of node i is given by the vector $x_i \in \mathbb{R}^n$, the internal dynamics are described by $f(x_i)$, and the couplings $g(x_i, x_j)$ depend on the states of the interacting nodes [1]. The time delays τ_{ij} account for signal propagation and processing times. The coupling structure of the system is captured by a weighted directed graph described by the N -dimensional adjacency matrix $A_N = [a_{ij}]$ whose elements are defined as $a_{ij} \neq 0$

if node j is connected to node i and $a_{ij} = 0$ otherwise for $i, j = 1, \dots, N$. Our goal is to decompose the dynamics of (1) around an equilibrium and define modal coordinates in which the system becomes uncoupled and the corresponding modal equations can be analyzed separately by current state-of-the-art tools [6, 15, 27].

In this paper, for the sake of simplicity, we focus on the dynamics in the vicinity of the synchronous/uniform equilibrium $x_i(t) \equiv x^*$, $i = 1, \dots, N$ [2]. We define the perturbations $y_i = x_i - x^*$ for $i = 1, \dots, N$, so the linearization of (1) can be written as

$$\dot{y}_i(t) = L y_i(t) + R \sum_{j=1}^N a_{ij} y_j(t - \tau_{ij}). \quad (2)$$

The n -dimensional matrices L, R are given by

$$L = \partial f(x^*) + m \partial_1 g(x^*, x^*), \quad R = \partial_2 g(x^*, x^*), \quad (3)$$

where ∂_1 and ∂_2 represent partial derivatives with respect to the first and second set of variables, respectively, while $m = \sum_{j=1}^N a_{ij}$ is the (constant) row sum [2].

Using the notation $\mathbf{y} = \text{col}[y_1 \ y_2 \ \dots \ y_N] \in \mathbb{R}^{nN}$ the linear system (2) can be rewritten as

$$\dot{\mathbf{y}}(t) = (I_N \otimes L) \mathbf{y}(t) + (\mathcal{A}_N \otimes R) \mathbf{y}(t), \quad (4)$$

where I_N is the N -dimensional identity matrix while $\mathcal{A}_N = [a_{ij} \mathcal{S}_{-\tau_{ij}}]$ is an adjacency operator that incorporates the components of the adjacency matrix as well as the time-shift operator

$$\mathcal{S}_{-\tau_{ij}} y_j(t) = y_j(t - \tau_{ij}). \quad (5)$$

In order to decompose system (4) into N modes of size n , one needs to diagonalize the adjacency operator \mathcal{A}_N . First, we take the Laplace transform of (4) and neglect the terms that would arise from a particular initial condition:

$$s \mathbf{Y}(s) = (I_N \otimes L) \mathbf{Y}(s) + (B_N(s) \otimes R) \mathbf{Y}(s), \quad (6)$$

where the matrix $B_N(s) = [a_{ij} e^{-s \tau_{ij}}]$ is the Laplace transform of the adjacency operator \mathcal{A}_N [3, 33]. Then we define the modal transformation

$$\mathbf{Y}(s) = (T_N(s) \otimes I) \mathbf{Z}(s), \quad (7)$$

where the columns of the matrix $T_N(s)$ consist of the eigenvectors of $B_N(s)$. This yields

$$s \mathbf{Z}(s) = (I_N \otimes L) \mathbf{Z}(s) + (C_N(s) \otimes R) \mathbf{Z}(s), \quad (8)$$

where $\mathbf{Z}(s)$ is the Laplace transform of the vector $\mathbf{z} = \text{col}[z_1 \ z_2 \ \dots \ z_N] \in \mathbb{R}^{nN}$ and the diagonal matrix $C_N(s)$ contains the eigenvalues $\Lambda_k(s)$ of $B_N(s)$. That is, the node-size modal equations in the Laplace domain become uncoupled:

$$s Z_k(s) = L Z_k(s) + R \Lambda_k(s) Z_k(s), \quad (9)$$

for $k = 1, \dots, N$. We remark that even if the adjacency matrix A_N is not diagonalizable (i.e., it has eigenvalues whose algebraic multiplicity is larger than their geometric multiplicity), the matrix $B_N(s)$ in (6) may still be diagonalized, that is, heterogeneity in the delays can destroy the symmetry imposed by the coupling structure.

The inverse Laplace transform of (9) results in the distributed delay systems

$$\dot{z}_k(t) = L z_k(t) + R \int_0^t \lambda_k(\xi) z_k(t - \xi) d\xi, \quad (10)$$

in the time domain where $\lambda_k(\xi)$ is the inverse Laplace transform of $\Lambda_k(s)$ for $k = 1, \dots, N$. We remark that the infinite dimensionality of transformation $T_N(s)$ in (7) can be understood by observing that it ‘‘shuffles’’ the present and past values of the coordinates in the time domain.

The stability of the modal equations (10) can be analyzed by the direct methods given in [31] or by obtaining $\lambda_k(\xi)$ using inverse Laplace transform. Note that the eigenvalues can be written as

$$\Lambda_k(s) = \bar{\Lambda}_k(e^{-s \tau_{11}}, e^{-s \tau_{12}}, \dots, e^{-s \tau_{NN}}). \quad (11)$$

In general $\bar{\Lambda}_k$ is a nonlinear function and $e^{-s \tau_{ij}}$ are periodic along the contour $s = i\omega$, which makes (11) quasi-periodic with frequencies τ_{ij} . Furthermore, the inverse Laplace transform is equivalent to the Fourier transform [19], that takes quasi-periodic functions into sums of periodic functions with frequencies from the set $\Omega = \{\sum_{ij} p_{ij} \tau_{ij} \geq 0 : p_{ij} \in \mathbb{Z}\}$. Therefore the eigenvalues can be approximated as

$$\Lambda_k(s) \approx \sum_{\ell: T_{k,\ell} \in \Omega} \rho_{k,\ell} e^{-s T_{k,\ell}}, \quad (12)$$

where the coefficients are calculated by truncating the Fourier transform

$$\rho_{k,\ell} = \lim_{T \rightarrow \infty} \frac{1}{T} \int_0^T \Lambda_k(i\omega) e^{i\omega T_{k,\ell}} d\omega. \quad (13)$$

If $\bar{\Lambda}_k$ in (11) is a smooth function of its variables, more insight can be gained by using multi-variable Taylor expansion about a point where all the variables assume the value $e^{-s T_0}$ (identical delays $\tau_{ij} = T_0$) [29]. The corresponding coefficients can be obtained by calculating the partial derivatives $\partial_1^{q_1} \dots \partial_M^{q_M} \bar{\Lambda}_k(e^{-s T_0}, \dots, e^{-s T_0}) = e^{(Q-1)s T_0} \Phi_{k,q_1 \dots q_M}$ where $M = N^2$ is the number of variables, $Q = q_1 + \dots + q_M$ is the order of the derivative, and $\Phi_{k,q_1 \dots q_M}$ only depend on the coupling strengths a_{ij} , hence they are independent of s [5]. Choosing $T_0 = \min\{\tau_{ij}\}$ guarantees that all the resulting exponential terms are in the form of $e^{-s T_{k,\ell}}$ with non-negative $T_{k,\ell} \in \Omega$, which is required by causality. The clear advantage of the Taylor expansion over the integral method is that it is more likely to provide analytical results in some simple cases.

The inverse Laplace transform of $e^{-sT_{k,\ell}}$ is the Dirac delta $\delta(\xi - T_{k,\ell})$, that is, (12) results in the distribution

$$\lambda_k(\xi) \approx \sum_{\ell: T_{k,\ell} \in \Omega} \rho_{k,\ell} \delta(\xi - T_{k,\ell}). \quad (14)$$

Thus, the convolution integral in (10) can be evaluated yielding the delay equations

$$\dot{z}_k(t) = L z_k(t) + R \sum_{\ell: T_{k,\ell} \in \Omega} \rho_{k,\ell} z_k(t - T_{k,\ell}), \quad (15)$$

for $k = 1, \dots, N$, which approximate distributed delays by (infinitely many) discrete delays. The stability of the equilibrium can be studied using the approximate characteristic equations

$$\det(sI - L - R \sum_{\ell: T_{k,\ell} \in \Omega} \rho_{k,\ell} e^{-sT_{k,\ell}}) = 0, \quad (16)$$

where I is the n -dimensional identity matrix. Considering $s = i\omega$, $\omega \geq 0$ the stability boundaries can be derived analytically [15], while discretizing time in (10) or (15) may allow numerical approximation of the characteristic roots s [27].

To gain insight to the physics of connected vehicle systems and to illustrate our above derived formalism we consider a simple car-following model. Car-following models describe the motion of individual vehicles moving in continuous time and space [12, 25]. These models can be extended to incorporate vehicle-to-vehicle (V2V) communication which changes the network structure by introducing long range connections with heterogenous delays.

We consider a simplified model with node dimension $n = 1$, where only the vehicles' speed v_i , $i = 1, \dots, N$ are exchanged via communication:

$$\dot{v}_i(t) = \gamma(v_0 - v_i(t)) + \sum_{j=1}^N \beta_{ij} V(v_j(t - \tau_{ij}) - v_i(t)). \quad (17)$$

Here V is a monotonously increasing function with $V(0) = 0$, while γ and β_{ij} represent the gains to maintain the desired velocity v_0 and zero relative velocity, respectively. We consider periodic boundary conditions, i.e., put the vehicles on a ring road. It can be shown analytically that the linear stability conditions obtained for large N are equivalent to the conditions that guarantee attenuation of perturbations along vehicle platoons [25]. For the sake of simplicity here we restrict ourselves to the simplest nontrivial case of $N = 3$ vehicles; see Fig. 1(a). Also, we consider the coupling constants $\beta_{ii} = 0$ and $\beta_{ij} = \beta$ for $i \neq j$ and the heterogenous delay setup $\tau_{ij} = \tau$ for $i \neq j$ except $\tau_{32} = \sigma \geq \tau$. This mimics the scenario that vehicle 1 obstructs the transmission of information from vehicle 2 to vehicle 3, resulting in longer delay.

By linearizing (17) about the uniform equilibrium $v_i(t) \equiv v_0$, $i = 1, 2, 3$ we obtain the linear system

$$\begin{bmatrix} \dot{\tilde{v}}_1(t) \\ \dot{\tilde{v}}_2(t) \\ \dot{\tilde{v}}_3(t) \end{bmatrix} = a \underbrace{\begin{bmatrix} 1 & 0 & 0 \\ 0 & 1 & 0 \\ 0 & 0 & 1 \end{bmatrix}}_{I_N} \begin{bmatrix} \tilde{v}_1(t) \\ \tilde{v}_2(t) \\ \tilde{v}_3(t) \end{bmatrix} + b \underbrace{\begin{bmatrix} 0 & \mathcal{S}_{-\tau} & \mathcal{S}_{-\tau} \\ \mathcal{S}_{-\tau} & 0 & \mathcal{S}_{-\tau} \\ \mathcal{S}_{-\tau} & \mathcal{S}_{-\sigma} & 0 \end{bmatrix}}_{\mathcal{A}_N} \begin{bmatrix} \tilde{v}_1(t) \\ \tilde{v}_2(t) \\ \tilde{v}_3(t) \end{bmatrix} \quad (18)$$

where $\tilde{v}_i = v_i - v_0$, $a = -\gamma - 2\beta V'(0)$ and $b = \beta V'(0)$.

To decompose (18) into its modal components we calculate the Laplace transform of the adjacency operator \mathcal{A}_N :

$$B_N(s) = \begin{bmatrix} 0 & e^{-s\tau} & e^{-s\tau} \\ e^{-s\tau} & 0 & e^{-s\tau} \\ e^{-s\tau} & e^{-s\sigma} & 0 \end{bmatrix}, \quad (19)$$

cf. (6), which possesses the eigenvalues

$$\begin{aligned} \Lambda_{1,2}(s) &= \frac{1}{2}(e^{-s\tau} \pm \sqrt{5e^{-2s\tau} + 4e^{-s(\tau+\sigma)}}), \\ \Lambda_3(s) &= -e^{-s\tau}, \end{aligned} \quad (20)$$

that appear in the modal equations (9) in the Laplace domain. To approximate the convolution by discrete delays in the modal equations (10) in the time domain we calculate the Taylor expansion of $\bar{\Lambda}_{1,2}(x, y) = \frac{1}{2}(x \pm \sqrt{5x^2 + 4xy})$ about (x_0, y_0) and then set $x_0 = y_0 = e^{-s\tau}$; cf. (11) and the discussion after (13). The resulting expression is a polynomial in $e^{-s\tau}$ and $e^{-s\sigma}$. Calculating the inverse Laplace transform we obtain the modal equations

$$\begin{aligned} \dot{\tilde{w}}_k(t) &= a \tilde{w}_k(t) + b \sum_{\ell=0}^K \rho_{k,\ell} \tilde{w}_k(t - T_{k,\ell}), \quad k = 1, 2, \\ \dot{\tilde{w}}_3(t) &= a \tilde{w}_3(t) - b \tilde{w}_3(t - \tau), \end{aligned} \quad (21)$$

where the support of the delay distributions is given by

$$T_{k,\ell} = \ell\sigma - (\ell - 1)\tau, \quad (22)$$

for $k = 1, 2$. In Fig. 1(b) dash-dotted blue lines with circles and solid red lines with crosses show the delay distributions for modes 1 and 2, respectively, for $K = 6$. These analytical results are approximated very well by the distributions obtained numerically using (13) that are shown as solid gray curves. We used $T = 1000\tau$ and $p_1, p_2 = -20, \dots, 20$ so that $T_{k,\ell} = p_1\tau + p_2\sigma \geq 0$.

The modal equations (21) result in the characteristic equations

$$\begin{aligned} s - a - b \sum_{\ell=0}^K \rho_{k,\ell} e^{-sT_{k,\ell}} &= 0, \quad k = 1, 2, \\ s - a + b e^{-s\tau} &= 0. \end{aligned} \quad (23)$$

Substituting $s = i\omega$, $\omega \geq 0$ we obtain the stability boundaries in the (a, b) -plane in parametric form for each mode. These are shown in Fig. 1(c) where modes are

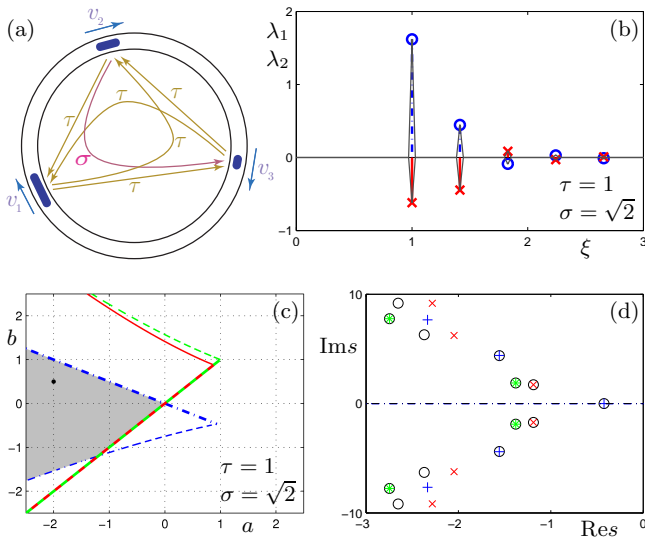


FIG. 1: (Color online) (a) A sketch of three vehicles following each other on a ring-road. Orange and purple arrows show the direction of information propagation through V2V communication with delays marked on each link. (b) Delay distributions (14) with support (22) for modes $k = 1, 2$. Dash-dotted blue lines with circles and solid red lines with crosses correspond to the distributions calculated analytically for modes 1 and 2, respectively. Numerical approximations are shown as solid gray curves. (c) Stability chart with the stable domain shaded. Dash-dotted blue, solid red and dashed green curves correspond to the 1st, 2nd and 3rd modes, respectively. When crossing thin curves stability changes through a pair of complex conjugate characteristic roots while thick lines correspond to stability change with zero characteristic root. (d) Comparing the leading characteristic roots obtained from (18) (black circles) and (21) (blue plus, red cross, green star for modes 1,2,3) for $K = 6$. Parameters correspond to the point marked by a dot on panel (c).

distinguished by color and line type (see caption). Thin curves correspond to $\omega > 0$ while thick lines correspond to $\omega = 0$. When crossing a thin curve, oscillations arise with frequency ω while crossing a thick line leads to non-oscillatory stability loss. (In the corresponding nonlinear system (17), Hopf and fold bifurcations take place.) Indeed, the equilibrium is stable if all modes are stable as indicated by the shaded domain. The accuracy of the stability boundaries improve when increasing the number of delays K in (23).

When discretizing time in systems (18) and (21), one may calculate the characteristic roots s numerically. Fig. 1(d) compares the characteristic roots for $K = 6$ for the parameter values corresponding to the dot in panel (c). Circles represent the characteristic roots obtained for (18) while other symbols represent the characteristic roots obtained for the individual modes in (21); see caption. Notice that the leading characteristic roots are reproduced very well while deviations occur for characteristic roots with smaller negative real part [4].

In order to evaluate the effects of delay heterogeneity on the system dynamics we depict the stability charts

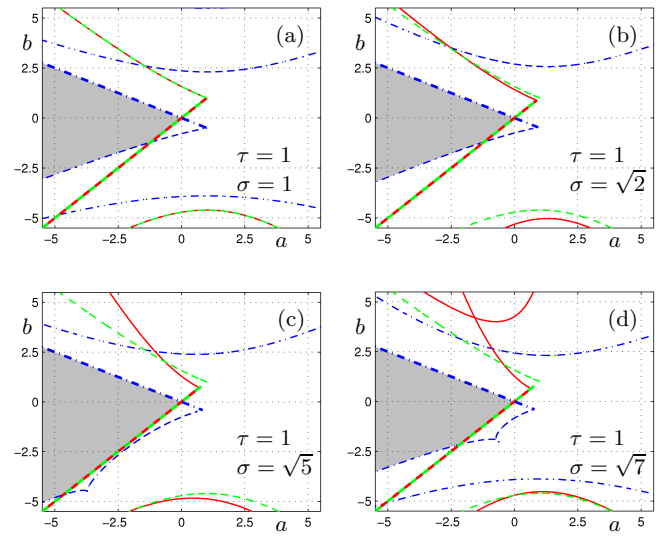


FIG. 2: (Color online) Stability charts with different delay values as indicated on each panel. The same notation is used as in Fig. 1(c).

for different σ values in Fig. 2. Using a larger parameter window compared to Fig. 1(c) reveals other stability curves (belonging to higher values of ω). Crossing these only makes the system “more unstable” with more characteristic roots on the right hand side. As can be seen in Fig. 2(a) the stability boundaries for modes 2 and 3 become identical when $\sigma = \tau$. In this case mode 1 is called tangential mode: when instability occurs in this mode the synchronous/uniform configuration is kept. On the other hand, modes 2 and 3 are transversal modes: stability losses in these modes breaks synchrony [21], leading to traveling waves. Such categorization is not possible for heterogeneous delays. In this case, each mode gives a different set of curves (see Fig. 2(b,c,d)) that correspond to different spatiotemporal patterns: traveling waves that are asymmetric due to the delays. Notice that as the heterogeneity in the delays increases the stable domain may increase or decrease in the (a, b) parameter plane. In fact, choosing the level of delay heterogeneity appropriately one may maximize the stable domain and so increase the robustness of the uniform flow.

In summary, this Rapid Communication introduced a new method in analyzing complex systems with coupling-delay heterogeneity that can be followed in a range of applications. In the vicinity of the synchronized equilibrium, through an infinite-dimensional modal transformation, modal equations with distributed delays were derived for heterogeneous delayed networks so that the spatiotemporal complexity of the network is embedded in the delay distributions. The analysis of the modal equations provide a systematic way to map out the system-level dynamics. It was demonstrated that the method can be used to analyze the spatiotemporal dynamics of connected vehicle systems. It was found that having appropriate level of delay heterogeneity can maximize the robustness of the uniform traffic flow.

Our future research we will extend these results using more realistic car-following models and connectivity structures. Indeed, applications extend beyond this specific problem. For example, one may extend the current framework to non-synchronized equilibria that can be used to design gene regulatory circuits of given functional properties [24]. Also, extending the framework to periodic orbits may allow one to characterize self-organized

criticality in neural networks [21, 22], which can lead to better understanding of neuro-computation and memory in the brain.

The authors greatly acknowledge the suggestions of Tamás Insperger, Gábor Stépán, and the two anonymous referees. We also thank Wubing Qin for his help with one of the figures.

-
- [1] (N1), The decomposition method is presented for the case where the node dynamics f are and the couplings g are uniform to reduce the algebraic complexity. Generalization for heterogeneous f and g will follow in future work.
- [2] (N2), The synchronized equilibrium x^* can be obtained by solving the algebraic equation $0 = f(x^*) + m g(x^*, x^*)$. The row sum $m = \sum_{j=1}^N a_{ij}$ must be the same for every i to ensure the existence of synchronous solutions.
- [3] (N3), Spelling out the terms arising from the initial conditions increases algebraic complexity without revealing additional physical features.
- [4] (N4), When the number of delays K is increased the leading characteristic roots are reproduced with higher accuracy, but accuracy may decrease for characteristic roots with smaller real part.
- [5] (S1), See Supplemental Material at [URL will be inserted by publisher] for calculating the derivatives of the eigenvalues $\bar{\Lambda}_k$.
- [6] Atay, F. M. (2003), *Physical Review Letters* **91** (9), 094101.
- [7] Campbell, S. A., and I. Kozlovskiy (2012), *Discrete and Continuous Dynamical Systems* **32** (8), 2653.
- [8] Caveney, D. (2010), *IEEE Control Systems Magazine* **30** (4), 38.
- [9] Cepeda-Gomez, R., and N. Olgac (2011), *IEEE Transactions on Automatic Control* **56** (7), 1734.
- [10] Choe, C.-U., T. Dahms, P. Hövel, and E. Schöll (2010), *Physical Review E* **81** (2), 025205.
- [11] Flunkert, V., S. Yanchuk, T. Dahms, and E. Schöll (2010), *Physical Review Letters* **105** (25), 254101.
- [12] Helbing, D. (2001), *Reviews of Modern Physics* **73** (4), 1067.
- [13] Hod, S. (2010), *Physical Review Letters* **105** (20), 208701.
- [14] Hunt, D., G. Korniss, and B. K. Szymanski (2010), *Physical Review Letters* **105** (6), 068701.
- [15] Insperger, T., and G. Stépán (2011), *Semi-discretization for Time-delay Systems: Stability and Engineering Applications*, Applied Mathematical Sciences, Vol. 178 (Springer).
- [16] Josic, K., J. M. López, W. Ott, L. Shiau, and M. R. Bennett (2011), *PLoS Computational Biology* **7** (11), e1002264.
- [17] Kantner, M., and S. Yanchuk (2013), *Philosophical Transactions of the Royal Society A* **371** (1999), 20120470.
- [18] Kinzel, W., A. Englert, G. Reents, M. Zigzag, and I. Kanter (2009), *Physics Review E* **79** (5), 056207.
- [19] Kuhlman, K. L. (2013), *Numerical Algorithms* **63** (2), 339.
- [20] Olfati-Saber, R., and R. M. Murray (2004), *IEEE Transactions on Automatic Control* **49** (9), 1520.
- [21] Orosz, G. (2013), in *Delay Systems: From Theory to Numerics and Applications*, edited by T. Vyhlýdal, J.-F. Lafay, and R. Sipahi (Springer) pp. 343–357.
- [22] Orosz, G. (2013), *SIAM Journal on Application of Dynamical Systems* **in review**.
- [23] Orosz, G., J. Moehlis, and F. Bullo (2010), *Physical Review E* **81** (2), 025204(R).
- [24] Orosz, G., J. Moehlis, and R. M. Murray (2010), *Philosophical Transactions of the Royal Society A* **368** (1911), 439.
- [25] Orosz, G., R. E. Wilson, and G. Stépán (2010), *Philosophical Transactions of the Royal Society A* **368** (1928), 4455.
- [26] Orosz, G., R. E. Wilson, R. Szalai, and G. Stépán (2009), *Physical Review E* **80** (4), 046205.
- [27] Roose, D., and R. Szalai (2007), in *Numerical Continuation Methods for Dynamical Systems*, Understanding Complex Systems, edited by B. Krauskopf, H. M. Osinga, and J. Galan-Vioque (Springer) pp. 359–399.
- [28] Safety Pilot, (2012), <http://safetypilot.umtri.umich.edu/>.
- [29] Scheidemann, V. (2005), *Introduction to Complex Analysis in Several Variables* (Birkhäuser).
- [30] Soriano, M. C., J. García-Ojalvo, C. R. Mirasso, and I. Fischer (2013), *Reviews of Modern Physics* **85** (1), 421470.
- [31] Stépán, G. (1989), *Retarded Dynamical Systems: Stability and Characteristic Functions*, Pitman Research Notes in Mathematics, Vol. 210 (Longman).
- [32] Treiber, M., A. Kesting, and D. Helbing (2006), *Physica A* **360** (1), 71.
- [33] Yi, S., P. W. Nelson, and A. G. Ulsoy (2010), *Time Delay Systems: Analysis and Control Using the Lambert W Function* (World Scientific).